Pharmacological Research 169 (2021) 105492

Contents lists available at ScienceDirect

Pharmacological Research

journal homepage: www.elsevier.com/locate/yphrs

(+)-trans-Cannabidiol-2-hydroxy pentyl is a dual CB_1R antagonist/CB_2R agonist that prevents diabetic nephropathy in mice

Isabel González-Mariscal [a,*], Beatriz Carmona-Hidalgo [b], Matthias Winkler [c], Juan D. Unciti-Broceta [b], Alejandro Escamilla [d], María Gómez-Cañas [e], Javier Fernández-Ruiz [e], Bernd L. Fiebich [f], Silvana-Yanina Romero-Zerbo [a], Francisco J. Bermúdez-Silva [a,g], Juan A. Collado [h,i,j], Eduardo Muñoz [h,i,j,**]

[a] Instituto de Investigación Biomédica de Málaga-IBIMA, UGC Endocrinología y Nutrición, Hospital Regional Universitario de Málaga, 29009 Málaga, Spain
[b] Emerald Health Biotechnology, Córdoba, Spain
[c] Symrise AG, Holzminden, Germany
[d] Microscopy platform, IBIMA, Malaga, Spain
[e] Departamento de Bioquímica y Biología Molecular, Facultad de Medicina, Instituto Universitario de Investigación en Neuroquímica, Universidad Complutense, CIBERNED and IRYCIS, Madrid, Spain
[f] VivaCell Biotechnology GmbH, Dezlingen, Germany
[g] Centro de Investigación Biomédica en Red de Diabetes y Enfermedades Metabólicas Asociadas (CIBERDEM), Madrid, Spain
[h] Instituto Maimónides de Investigación Biomédica de Córdoba, Spain
[i] Departamento de Biología Celular, Fisiología e Inmunología, Universidad de Córdoba, 14004 Córdoba, Spain
[j] Hospital Universitario Reina Sofía, Córdoba, Spain

ARTICLE INFO

Keywords:
Cannabidiol
(+)-enantiomers
Cannabinoids
Cannabinoid 1 receptor
Cannabinoid 2 receptor
Diabetic nephropathy
Type 1 diabetes

ABSTRACT

Natural cannabidiol ((-)-CBD) and its derivatives have increased interest for medicinal applications due to their broad biological activity spectrum, including targeting of the cannabinoid receptors type 1 (CB_1R) and type 2 (CB_2R). Herein, we synthesized the (+)-enantiomer of CBD and its derivative (+)-CBD hydroxypentylester ((+)-CBD-HPE) that showed enhanced CB_1R and CB_2R binding and functional activities compared to their respective (-) enantiomers. (+)-CBD-HPE *Ki* values for CB_1R and CB_2R were 3.1 ± 1.1 and 0.8 ± 0.1 nM respectively acting as CB_1R antagonist and CB_2R agonist. We further tested the capacity of (+)-CBD-HPE to prevent hyperglycemia and its complications in a mouse model. (+)-CBD-HPE significantly reduced streptozotocin (STZ)-induced hyperglycemia and glucose intolerance by preserving pancreatic beta cell mass. (+)-CBD-HPE significantly reduced activation of NF-κB by phosphorylation by 15% compared to STZ-vehicle mice, and $CD3^+$ T cell infiltration into the islets was avoided. Consequently, (+)-CBD-HPE prevented STZ-induced apoptosis in islets. STZ induced inflammation and kidney damage, visualized by a significant increase in plasma proinflammatory cytokines, creatinine, and BUN. Treatment with (+)-CBD-HPE significantly reduced 2.5-fold plasma IFN-γ and increased 3-fold IL-5 levels compared to STZ-treated mice, without altering IL-18. (+)-CBD-HPE also significantly reduced creatinine and BUN levels to those comparable to healthy controls. At the macroscopy level, (+)-CBD-HPE prevented STZ-induced lesions in the kidney and voided renal fibrosis and $CD3^+$ T cell infiltration. Thus, (+)-enantiomers of CBD, particularly (+)-CBD-HPE, have a promising potential due to their pharmacological profile and synthesis, potentially to be used for metabolic and immune-related disorders.

Abbreviations: CBD, Cannabidiol; CB1R and CB2R, Cannabinoid receptors type 1 and 2; NAM, Negative allosteric modulator; T1D, Type 1 diabetes; NOD, Non-obese diabetic mice; CRE, cAMP response element; STZ, Streptozotocin; PAS, Periodic Acid Schiff; PSR, Picrosirius Red staining; BSA, Bovine serum albumin; BUN, Blood urea nitrogen.

* Corresponding author.
** Corresponding author at: Departamento de Biología Celular, Fisiología e Inmunología, Universidad de Córdoba,14004 Córdoba, Spain.
E-mail addresses: isabel.gonzalez@ibima.eu (I. González-Mariscal), fi1muble@uco.es (E. Muñoz).

https://doi.org/10.1016/j.phrs.2021.105492
Received 23 November 2020; Received in revised form 21 January 2021; Accepted 11 February 2021
Available online 19 May 2021

1. Introduction

The most occurring non-psychotropic cannabinoid found in *Cannabis sativa*, cannabidiol (CBD), has increased interest for medicinal applications due to its broad biological activity spectrum (reviewed in [1]). The use of CBD preparations is becoming popular with dozens of products already in the market claiming different health benefits based on anecdotal evidence. More importantly, CBD is used in combination with $^{9}\Delta$-Tetrahydrocannabinol (Sativex®) for the treatment of spasticity in multiple sclerosis patients, and as a single drug (Epidiolex®) for the treatment of refractory epilepsies in children [2,3]. A large number of marketed drugs are based or inspired by natural products. This, numerous CBD derivatives (*e.g.* fluorinated, hydroxyquinones, methyl-ester, *etc.*) have been generated to improve its pharmacological properties [1].

The mechanism of action of CBD is not completely understood and the signaling through canonical cannabinoid receptors type 1 and 2 (CB_1R and CB_2R) has been controversial. Nevertheless, CBD does not bind to the orthosteric site of CB_1R and it has been proposed that act as a negative allosteric modulator (NAM) of CB_1R, which may explain some of the biological activities mediated by this cannabinoid [4].

Naturally occurring CBD has the absolute stereo conformation (-)-trans. Cis-isomers or (+)-enantiomers are not produced in plants and have, therefore, until now, no pharmaceutical impact. However, the synthetic enantiomer (+)-trans-CBD binds to CB_1R and CB_2R at nanomolar concentrations [5] but did not exhibit any effects in the tetrad group of assays (ambulation, sedation, analgesia, temperature lowering), which are typical for cannabinoid CB_1R agonists [6]. Therefore, it is possible that (+)-trans-CBD does not penetrate the brain or, more likely, does not behave as a full CB_1R agonist. Interestingly, (+)-trans-CBD has been used as a template to develop novel derivatives with enhancing binding affinity to CB_1R and CB_2R. Among them, (+)-Cannabidiol-dimethyl heptyl have shown to exert analgesic activity [6,7].

We have recently shown that chemical modifications of (-)-CBD at position 2 of the resorcinol moiety increased the binding of both CB_1R and CB_2R. Thus, (-)-CBD-2-hydroxy pentyl ((-)-CBD-HPE) showed a strong binding for CB_2R and a moderate binding to CB_1R. In functional assays (-)-CBD-HPE behaved as an agonist for CB_2R and antagonist for CB_1R [8]. Such pharmacological profile has been investigated for other natural and synthetic cannabinoids, as it is known to impact metabolism and immune action and has a great potential for the treatment of a wide range of diseases. Type 1 diabetes (T1D) is an autoimmune disease with no cure characterized by the infiltration of immune cells in and around the islets, leading to the progressive loss of beta cell mass and hyperglycemia [9]. High blood glucose due to T1D increases the risk of macro and microvascular complications, including renal failure [10]. CBD delayed the onset of T1D in non-obese diabetic mice (NOD) [11], but the impact of targeting CB_1R and CB_2R on T1D and its complications remains unstudied. Antagonism of CB_1R has been shown to alleviate nephropathy in type 2 diabetic rats [12], and blockade or genetic ablation of CB_1R preserves insulin-producing pancreatic beta cell viability and function and also prevents the infiltration of immune cells in and around pancreatic islets in obese mice [13,14]. CB_2R is mainly expressed in immune cells, and its agonism reduces ROS production, cytokine release, and immune cell proliferation [15].

In the present study, we first explored whether, as it happens with (+)-trans-CBD [5], the synthesis of the (+)-enantiomer of CBD-HPE is also accompanied by an increase in its binding activity on both CB_1R and CB_2R, as well as in its activity as CB_1R antagonist and CB_2R agonist. As a second objective, we have investigated the efficacy of this new (+)-CBD derivative to ameliorate nephropathy in a murine model of T1D.

2. Material and methods

2.1. Synthesis of (+)-CBD enantiomers

The schematic synthesis of (+)-CBD and (+)-CBD-HPE enantiomers is shown in Fig. 1.

2.1.1. Synthesis of (+)-CBD ME (1)

71.4 g (300 mM) olivetol methyl ester and 50 g (330 mM) 1 R,4S-menthadienol were dissolved together with toluene to reach a combined volume of 400 mL (Solution A). 21.3 g (150 mM) BF_3 etherate was dissolved with toluene to reach a volume of 300 mL (Solution B). Both reaction solutions were then put through two pump systems and the continuous flow reactor (rotation: 1200 U/min, solution A: 24 mL/min, solution B: 12 mL/min). Solution B started before and ended after solution A to guarantee that catalyst is always present in the reaction chamber. The reaction mixture was continuously collected in a 2-liter lab reactor (30 °C mantel temperature, 300 rpm) filled with a 700 mL saturated $NaHCO_3$ solution. The aqueous solution was discarded; the organic solution was washed at 45 °C 4 times with 250 mL of 1% NaOH solution. After washing, the organic solution was evaporated to dryness to give 94.58 g of raw (+)-CBD methyl ester (purity = 78%, yield 68%). The raw compound was used further without purification.

2.1.2. Synthesis of (+)-CBD (3)

49.2 g (103 mM) (+)-CBD ME (**1**) was dissolved at 60 °C in 250 mL ethylene glycol and poured in a 1 L lab reactor. 5.7 g potassium hydroxide was added, and the reaction mixture was started to heat under stirring to 120 °C and a vacuum of 500 mbar. Accumulated volatile side products were distilled off. After 2 h the reaction temperature was increased to 150 °C and the temperature was kept for additional 3 h. The reaction mixture was cooled to 80 °C, following addition of 400 mL water and 130 mL n-heptane. The temperature was further decreased to 40 °C, following the slow addition of 1.2 mL of 50% sulfuric acid (50%) until a pH of approx. 6. The layers were separated; the organic layer was washed once with 250 mL of water and once with 250 mL of sodium hydroxide solution (0.05%). The organic layer was dried over Na_2SO_4 and then evaporated to dryness. Yield: 30.3 g, GC purity: 53%. A sample of the reaction mixture was taken after 2 h at 120 °C, quenched with n-heptane and water and neutralized with sulfuric acid (10% w/w). The layers were separated, and the organic layer was evaporated to dryness. The crude (+)-CBD (3) was purified by flash chromatography (eluent system cyclohexane / ethyl acetate = 20 / 1 v/v), following crystallization from n-heptane. GC purity: 99.8%. Chiral GC analysis: enantiomeric excess 99% (for enantiomeric pure starting material and for starting materials with up to 5% 4R-menthadienol enantiomer). ^{1}H NMR (400 MHz, $CDCl_3$) δ 6.35 – 6.09 (m, 2H), 5.97 (s, 1H), 5.57 (dt, J = 2.8, 1.6Hz, 1H), 4.66 (p, J = 1.6 Hz, 2H), 4.56 (d, J = 2.0 Hz, 1H), 3.85 (ddp, J = 10.7, 4.5, 2.3 Hz, 1H), 2.48 – 2.41 (m, 2H), 2.38 (ddd, J = 10.6, 3.7 Hz, 1H), 2.30 – 2.17 (m, 1H), 2.09 (ddt, J = 17.9, 5.1, 2.4 Hz, 1H), 1.88 – 1.81 (m, 1H), 1.79 (dt, J = 2.6, 1.2 Hz, 3H), 1.78 – 1.72 (m, 1H), 1.65 (t, J = 1.1 Hz, 3H), 1.62 – 1.50 (m, 2H), 1.37 – 1.22 (m, 4H), 0.88 (t, J = 7.0 Hz, 3H). ^{13}C NMR (101 MHz, $CDCl_3$) δ 156.07, 153.90, 149.41, 143.06, 140.07, 124.12, 113.76, 110.84, 109.84, 108.00, 7.35, 77.03, 76.71, 46.15, 37.28, 35.48, 31.50, 30.64, 30.41, 28.41, 23.69, 22.55, 20.54, 14.05 (Supplementary Fig. 1A).

2.1.3. Synthesis of (+)-CBD-HPE (4)

10 g (24 mM) (+)-CBD ME (**1**) was dissolved at 60 °C in 250 mL 1,2-pentanediol and poured in a 1 L lab reactor. 1.1 g potassium hydroxide was added, and the reaction mixture was started to heat under stirring to 120 °C and a vacuum of 500 mbar. Accumulated volatile side products were distilled off. After 2 h the reaction mixture was cooled to 80 °C, following addition of 400 mL water and 130 mL n-hexane. The temperature was further decreased to room temperature and neutralized with sulfuric acid (10% w/w). The layers were separated; the organic

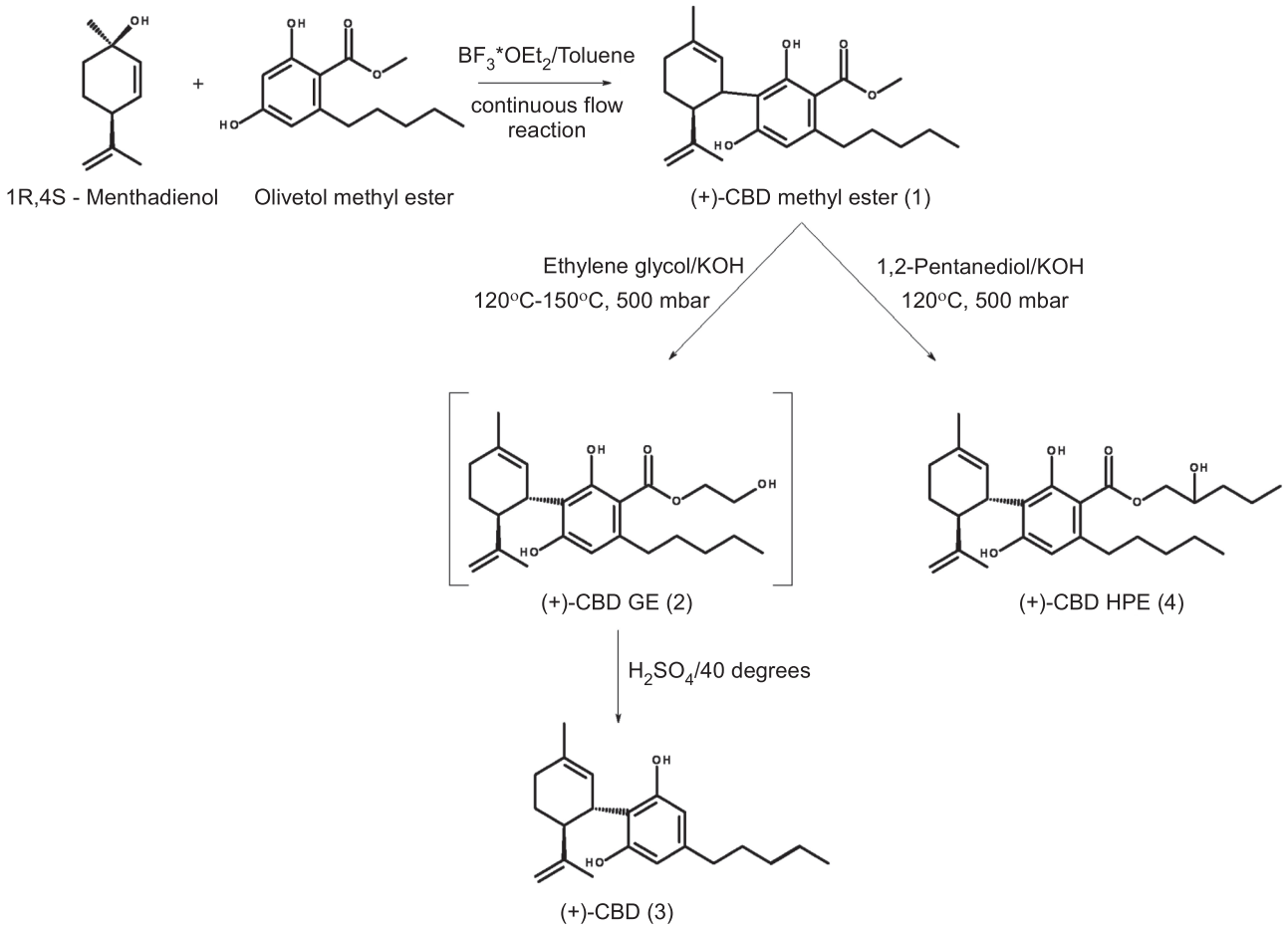

Fig. 1. Schematic representation of (+)-trans-CBD and (+)-CBD-HPE synthesis.

layer was washed once with 250 mL of water, dried over Na_2SO_4 and evaporated to dryness. The crude product (+)-CBD HPE (4) was purified by flash chromatography (eluent system cyclohexane / ethyl acetate = 10 / 1 v/v). GC purity: 98%. Chiral GC analysis: enantiomeric excess 99%. ^{1}H NMR (400 MHz, DMSO-d_6) δ 11.61 (s, 1H), 9.89 (s, 1H), 6.20 (s, 1H), 5.11 – 5.05 (m, 1H), 4.91 – 4.82 (m, 1H), 4.46 (d, J = 2.7Hz, 1H), 4.42 (dd, J = 2.8, 1.5 Hz, 1H), 4.24 – 4.11 (m, 2H), 3.95 – 3.86 (m, 1H), 3.81 – 3.71 (m, 1H), 3.03 (td, J = 11.4, 10.9, 3.0 Hz, 1H), 2.74 (s, 2H), 2.22 – 2.05 (m, 1H), 1.94 (dd, J = 16.7, 4.1 Hz, 1H), 1.76 – 1.63 (m, 2H), 1.61 (t, J = 1.8 Hz, 3H), 1.58 (s, 3H), 1.53 – 1.34 (m, 6H), 1.33 – 1.26 (m, 4H), 0.89 (t, J = 7.0 Hz, 3H), 0.86 (t, J = 6.7 Hz, 3H). ^{13}C NMR (101 MHz, DMSO-d_6) δ 171.22, 162.07, 160.33, 148.61, 144.07, 130.72, 125.60, 114.82, 110.15, 109.84, 103.50, 68.95, 67.27, 43.32, 35.71, 35.61, 35.44, 31.36, 30.91, 30.13, 29.12, 23.13, 22.00, 18.88, 18.12, 13.86, 13 (Supplementary Fig. 1B).

2.2. CB_1R and CB_2R binding assay

Binding assays were investigated by competition studies against [^{3}H] CP-55,940 (164.5 Ci/mmol, Perkin Elmer, Boston, MA, USA) to determine its binding affinity (Ki value) at both cannabinoid receptors using commercially available membranes prepared from CB_1R- or CB_2R-stably transfected HEK-293 cells (RBHCB1M400UA and RBXCB2M400UA, respectively; Perkin-Elmer) [16]. Briefly, membranes were added in assay buffer (for CB_1R: 50 mM Tris-Cl, 5 mM $MgCl_2{\cdot}H_2O$, 2.5 mM EDTA, 0.5 mg mL^{-1} bovine serum albumin, pH 7.4, or for CB_2R: 50 mM Tris-Cl, 5 mM $MgCl_2{\cdot}H_2O$, 2.5 mM EGTA, 1 mg mL^{-1} bovine serum albumin, pH 7.5) at a final concentration of 8 μg/well and 4 μg/well for CB_1R and for CB_2R receptors, respectively. The radioligand was used at 0.4 nM for CB_1R or 0.53 nM for CB_2R and in a final volume of 200 μl for both receptors. The reaction was stirred for 90 min at 30 °C. Non-specific binding was determined with non-radiolabeled WIN55,212-2 (Sigma Aldrich, 10 μM) in the presence of radioligand. 100% binding of the [^{3}H] CP-55,940 was determined by incubation of the membranes with radioligand in the absence of the tested cannabinoids. All of the plastic material employed was siliconized with Sigmacote (Sigma-Aldrich) to prevent possible adhesion of compounds. After incubation, free radioligand was separated from bound radioligand by filtration in GF/C filters, previously treated with a 0.05% (v v^{-1}) polyethylethylenimine solution. Then, filters were washed nine times with cold assay buffer, using the Harvester® filtermate equipment (Perkin Elmer). Radioactivity was measured using a liquid scintillation spectrometer (Microbeta Trilux 1450 LSC & Luminiscence Counter (Perkin Elmer)). Data were expressed as the percentage of [^{3}H]CP-55,940 binding. Ki values were obtained with GraphPad Prism (5.02) software (GraphPad Software Inc., San Diego, CA, USA).

2.3. Transfections and luciferase assays

HEK-293 T (8×10^4) cells stably expressing human cannabinoid CB_1R or CB_2R were seeded in 24-well plates and after 24 h were transiently transfected with the pCRE-Luc plasmid (0.2 μg/well) using Roti©-Fect (Carl Roth, Karlsruhe, Germany) following manufacturer's specifications. The CRE luciferase reporter contains the firefly luciferase gene under the control of the multimerized cAMP response element (CRE) located upstream of a minimal promoter. Twenty-four hours after transfection, CB_1R-HEK-293T cells were pretreated for 30 min with the cannabinoids and stimulated with WIN55,212 (1 μM) for 6 h. CB_2R-

HEK-293T cells were pretreated for 30 min with the cannabinoids or WIN55,212 as positive control and stimulated with Forskolin (FSK) (10 μM) for 6 h. After treatments, luciferase activity was measured using Dual-Luciferase Assay (Promega, Madison, WI, USA).

2.4. Animals

Animal care and procedures were approved by the Animal Experimentation Ethics Committee of the Malaga University and authorized by the government of Andalucia (Project number 28/06/2018/107), complied with the ARRIVE guidelines, and followed the EU Directive 2010/63/EU guidelines for animal experiments. C57BL6J mice (Charles River France) were housed in groups of 10 using 12 h dark/light cycles and provided food and water *ad libitum*. Eight- to 10-week-old C57BL6J male mice of 24.4 ± 0.2 g of body weight were randomized to 3 groups: healthy control (vehicle and citrate buffer), vehicle-streptozotocin (STZ), and (+)-CBD-HPE-STZ. Mice were injected daily intraperitoneally (i.p.) with vehicle (saline:DMSO:Tween-80, 95:4:1) or 10 mg/kg of (+)-CBD-HPE for 7 days. Mice were fasted for 4 h prior i.p. injections with STZ or citrate buffer (healthy controls) as described previously [17]. Mice were given 10% sucrose water for 48 h upon STZ treatment to prevent ongoing toxicity and to avoid hypoglycemia. Blood glucose was monitored daily using OneTouch Ultra blood glucose meter (LifeScan IP Holdings, LLC). After 6 days mice were euthanized by cervical dislocation, and tissues and blood were collected and processed immediately for histological and biochemical analysis.

2.5. Intraperitoneal glucose tolerance test

Mice were fasted overnight and given free access to water. Mice were given i.p. a bolus of 2 g/kg glucose and blood glucose was determined at 0, 15, 30, 60, and 90 min.

2.6. Tissue immunohistochemistry and histochemistry

Pancreas and kidney were dissected and fixed in methanol-free 4% paraformaldehyde (Pierce) for 6 h at room temperature or 24 h at 4 °C, respectively, prior paraffin embedding. Kidney sections (5 μm) were deparaffinized and dehydrated in a graded series (100–70%) of ethanol washes and stained with Periodic Acid Schiff (PAS) (Sigma-Aldrich, St. Louis, MO, USA) to evaluate renal pathology. Two independent assessors reviewed histological sections in a blinded manner and graded (0–3 scale) glomerular changes (hypercellularity, mesangial expansion, and capillary dilation, 40 glomeruli), tubular lesions (atrophy and degeneration, 20 fields at 40x magnification), and interstitial damage (fibrosis and inflammation, 20 fields at 40X magnification*) (PMID: 27609616)*. Imaging was performed using a light microscope Leica DM2000 microscope. Glomerular area and diameter were marked manually and calculated automatically using Image J software (http://rsb.info.nih.gov/.ij). Kidney collagen was detected by Picrosirius Red (PSR) staining (PSR) following the manufacturer's instructions (Sigma-Aldrich). Quantitative evaluation of PSR staining was estimated as the staining under a grid intersection / total number of intersections multiplied by 100 (% of the fraction area), as described previously [18]. The data were represented by the area percentage of each slide positive (20 fields at 40x magnification) for red stain which was calculated using Image J software. The mean scores were calculated by mouse and by group. For immunohistochemistry, heat-mediated citric acid- or EDTA-based for 20 min in a preheated steamer and a further 20 min of cooling down was performed. For DAB staining, peroxidase activity was blocked in 3% hydrogen peroxide for 10 min. For mouse-on-mouse staining, sections were pre-blocked with Rodent Block (Biocare Medical) for 30 min at room temperature and rinsed. Sections were blocked in 5% goat serum 0.3% Triton-X-100 in PBS or bovine serum albumin (BSA) 0.3% Triton-X-100 in PBS for phospho-antibodies for 30 min at 37 °C prior incubation with primary antibody in 1% serum or BSA, 0.3% Triton-X-100 in PBS overnight at 4 °C. Primary antibodies used were: mouse anti-insulin (SIGMA I-2018; 1:500), rabbit anti-NF-kB p65 phospho-S536 (Abcam ab86299; 1:100), rabbit anti-cleaved caspase 3 (Cell signaling 9661; 1:100) and mouse anti-CD3 (Santa Cruz Biotechnologies sc-20047; 1:50) for kidney and rabbit anti-CD3 (Abcam ab5690; 1:100) for pancreas. Sections were washed 3 times for 5 min in 0.3% Triton-X-100 PBS and incubated with secondary antibody in 1% serum or BSA, 0.3% Triton-X-100 in PBS for 30 min at 37 °C and then washed 3 times for 5 min in 0.3% Triton-X-100 PBS. Alexa Fluor or HRP polymer-conjugated antibodies were incubated for 45 min at 37 °C, and nuclei stained using DAPI for immunofluorescence. DAB staining was performed following hematoxylin for nuclei staining. Negative controls were performed using 0.3% Triton-X-100 PBS containing 1% goat serum or BSA. Imaging was performed at 20X using an Olympus BX41. The densitometry of images was analyzed using ImageJ (NIH). DAB staining was quantified using ImageJ Fiji after color deconvolution and further processed by Image J software to quantify signal intensity. Cell count was analyzed by a manual count of n = 100 islets per group.

2.7. Plasma proteins and nitrogen determination

Cytokines in plasma were determined using the multiplex assay ProcartaPlex Immunoassay (Thermo Fisher Scientific) designed for T1D following manufacturer's instructions. Cytokines bellow the standard curve were discarded as non-detected. Blood urea nitrogen (BUN) and creatinine were determined using DetectX BUN Detection Kit and DetectX Creatinine Serum Kit (Arbor Assays) following the manufacturer's instructions.

2.8. Randomization

Mice were randomly assigned to healthy control, vehicle-STZ, or (+)-CBD-HPE-STZ groups.

2.9. Blinding

Mice used in this study were assigned a numerical code and analysis blinded.

2.10. Statistical analysis

Data are shown as mean ± SEM. Statistical analysis was performed using GraphPad Prism version 6.07. Mean values were compared using ANOVA with Tukey's or Dunn's test for a parametric or non-parametric test, respectively. A p-value < 0.05 was considered significant.

3. Results

3.1. Binding and functional activities of (+) enantiomers on cannabinoid receptors

(+)-CBD and its derivatives (Fig. 1) were synthesized as described above, with 99–98% purity and an enantiomeric excess of 99% (see Supplementary Fig. 1 for NMR spectra). In order to characterize the (+)-CBD and its derivative (+)-CBD-HPE and to compare with synthetic (-)-CBD and (-)-CBD-HPE (2-HPC in [8]) we explored their binding capability to CB_1R and CB_2R. As shown in Table 1, (-)-CBD presented a

Table 1
Binding of (-) and (+)-enantiomers of CBD to CB_1R and CB_2R.

Compound	CB_1R-Ki (nM)	CB_2R-Ki (nM)	CB_1R/CB_2R selectivity
(-)-CBD	8960 ± 371	4310 ± 1292	2.1
(+)-CBD	982 ± 306	40.5 ± 7.3	24.3
(-)-CBD-HPE	538 ± 54	66.7 ± 13.1	8.1
(+)-CBD-HPE	3.1 ± 1.1	0.8 ± 0.1	3.9

low binding activity on both CB_1R and CB_2R (Table 1), and, as expected, the enantiomer (+)-CBD showed a higher binding activity for both receptors (Table 1). (-)-CBE-HPE showed an increased binding affinity CB_1R and CB_2R compared to (-)-CBD (data from [8]; Table 1). Importantly, (+)-CBE-HPE presented a very potent binding affinity for the cannabinoid receptors, with 2.9×10^3-fold and 5.3×10^3-fold higher affinity for CB_1R and CB_2R, respectively, than (-)-CBD, a 316-fold and a 50-fold increased affinity compared to (+)-CBD, and a 180-fold and 82-fold increased affinity compared to (-)-CBD-HPE (Table 1). Thus, we selected (+)-CBE-HPE to evaluate the functional activity on CB_1R and CB_2R signaling by luciferase assay in 293 T-CB1-CRE-Luc and 293 T-CB2-CRE-Luc cell lines. As depicted in Fig. 2A, (+)-CBE-HPE showed CB_2R agonistic activity starting at 100 nM (Fig. 2A), while it did not activate CB_1R at the concentrations tested (Fig. 2B). (+)-CBE-HPE showed a strong CB_1R antagonistic activity against WIN 55,212–2 compound, starting at 100 nM and with a full inactivation at 5 μM (Fig. 2C). The concentration-response curves showed values of IC50 for CB1R and EC50 for CB2R of 0.21 ± 0.07 and 0.09 ± 0.78 μmol/L, respectively.

3.2. (+)-CBD-HPE prevents STZ-induced hyperglycemia

Phyto- and synthetic cannabinoids have been shown to delay the onset of diabetes and alleviate inflammation in metabolic-related diseases; CB_1R has been proposed as a target for the treatment of metabolic disorders and antifibrotic treatments, and both CB_1R and CB_2R targets for the treatment for inflammation. Thus, we tested (+)-CBD-HPE in an experimental mouse model of T1D. Eight- to 10-week-old C57BL6J mice were pretreated with vehicle or 10 mg/kg of (+)-CBD-HPE for one-week, prior insult with STZ, a drug preferentially toxic to pancreatic beta cells, or citrate buffer (healthy control) (Fig. 3 A). Vehicle-STZ mice developed hyperglycemia 3 days after STZ injection (Fig. 3B). Mice treated with (+)-CBD-HPE did not become hyperglycemic, and blood glucose levels were significantly lower than those of vehicle-STZ mice and comparable to healthy control mice (Fig. 3B). On day 14, fasting blood glucose was significantly higher in vehicle-treated mice than healthy controls (114 ± 8 mg/dl *vs.* 89 ± 4 mg/dl, respectively). Mice pretreated with (+)-CBD-HPE had significantly lower fasting blood glucose (81 ± 5 mg/dl), comparable to healthy control. Vehicle-STZ mice were glucose intolerant as shown by higher blood glucose levels than healthy controls during an IPGTT (Fig. 3D-E). Pretreatment with (+)-CBD-HPE improved glucose tolerance in STZ-injected mice, as shown by lower blood glucose than vehicle-STZ mice during an IPGTT (Fig. 3D-E).

3.3. (+)-CBD-HPE alleviates STZ-induced pancreatic beta cell loss

STZ induces T1D by directly impacting insulin-producing beta cells, leading to loss of beta cell mass, hence hyperglycemia. Since (+)-CBD-HPE prevented STZ-induced hyperglycemia, we investigated the effect of (+)-CBD-HPE on beta cells. As described previously, STZ induced a significant 2.8-fold reduction of islet insulin content, as determined by insulin staining of the pancreas (Fig. 3F-G), and a loss of 78% of beta cell mass compared to healthy controls (Fig. 3H), accompanied by a significant 1.5-fold increase in islet area (Fig. 3I). Islets from mice pretreated with (+)-CBD-HPE had significantly more intra-islet insulin content than those from vehicle-STZ mice, and only a 1.6-fold reduction compared to healthy control (Fig. 3F-G). Importantly, (+)-CBD-HPE prevented STZ-induced beta cell mass loss (Fig. 3H). Islet area was significantly increased by 1.2-fold in (+)-CBD-HPE pretreated STZ-mice compared to healthy control (Fig. 3I).

3.4. (+)-CBD-HPE prevents STZ-induced inflammation

Damage in beta cells by STZ triggers islet inflammation [19], and beta cell mass loss is driven by activation of NF-κB in T1D [20]. Islets

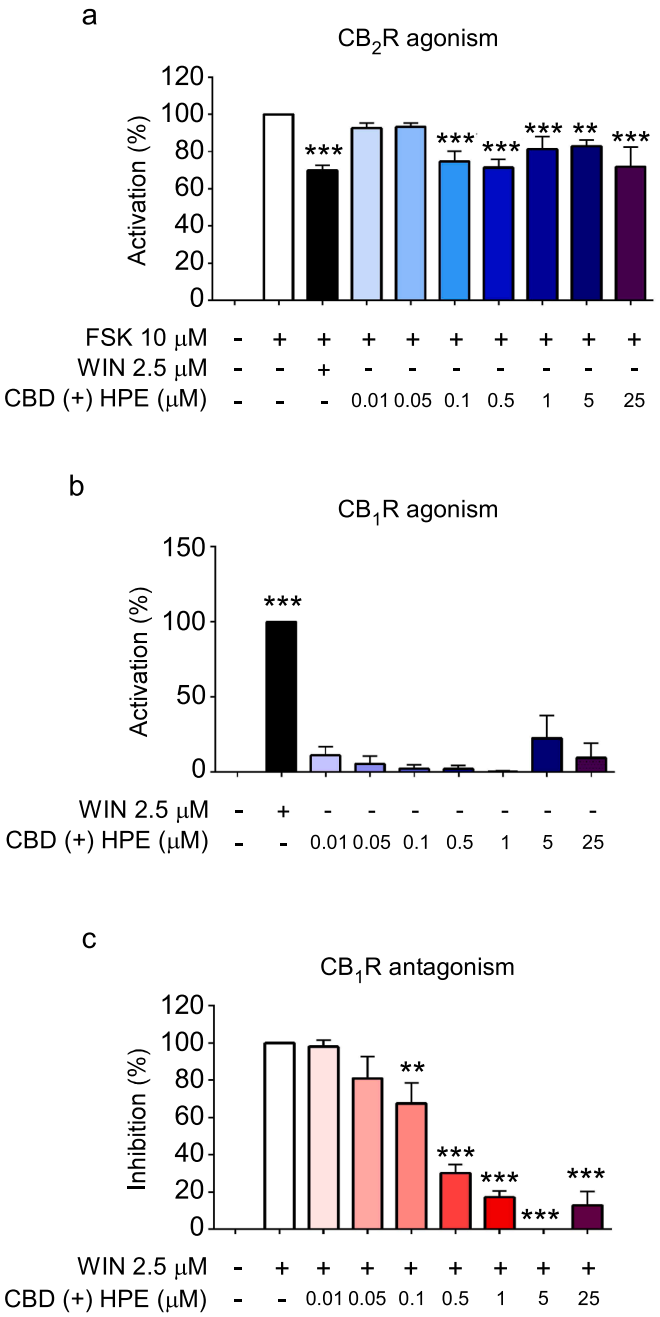

Fig. 2. Pharmacological evaluation of (+)-CBD-HPE. (a) hCB_2R receptor agonism. HEK-293T-CB_2-CRE-Luc cells were treated with WIN 55,212–2 (WIN) or (+)-CBD-HPE for 30 min and stimulated with FSK for 6 h. Then, cells were lysed for luciferase activity. Data are shown as mean activation percentage ± S. D. considering FSK as 100% activation. (n = 3). ***$p < 0.001$ *versus* FSK. (b) hCB_1R receptor agonism. HEK-293T-CB_1-CRE-Luc cells. were treated with WIN 55,212–2 (WIN) or (+)-CBD-HPE for 6 h and lysed for luciferase activity measurement. (c) hCB_1R receptor antagonism. Results of CB_1-CRELuc-HEK-293 cells pretreated with (+)-CBD-HPE and stimulated with WIN 55,212–2 for six hours. The effect of WIN 55,212–2 was considered a 100% activation. Results are shown as mean ± SD (n = 3). **$p < 0.01$ and ***$p < 0.001$ *versus* WIN 55,212–2.

from vehicle-STZ mice showed activation of NF-κB, determined by a 30% increase in its phosphorylation and nuclear localization compared to healthy control (Fig. 4A-B), which was prevented by (+)-CBD-HPE (Fig. 4A-B). Treatment with STZ triggered the infiltration of T cells into the islet, a process known as insulitis, as determined by a significant increase in the number of CD3 + cells (Fig. 4C-D). (+)-CBD-HPE

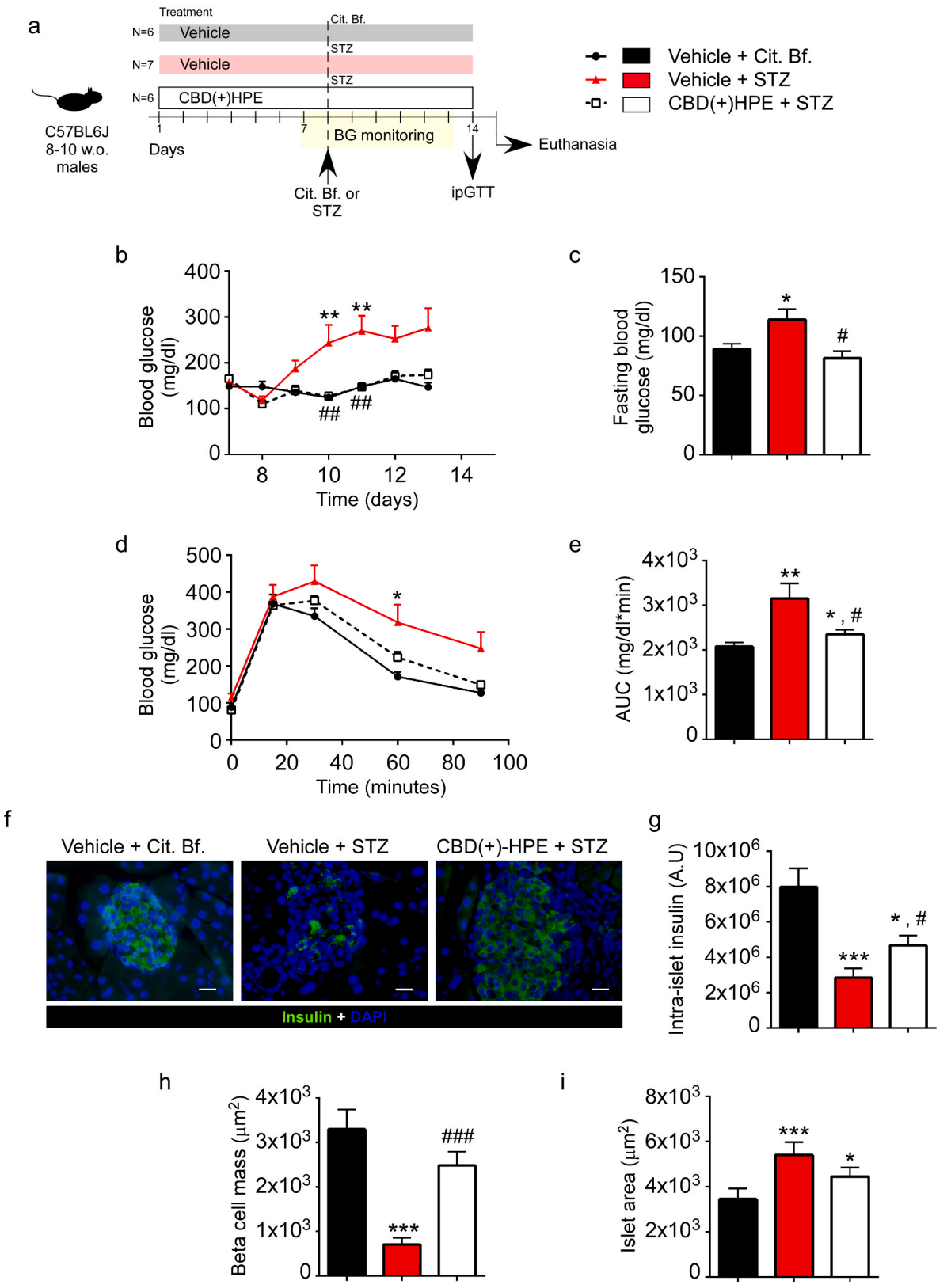

Fig. 3. (+)-CBD-HPE prevents STZ-induced hyperglycemia and protects beta cell mass. (a) Mice were treated with vehicle-citrate buffer (Vehicle-Cit. Bf.; black circles, solid line; black bars), vehicle-STZ (red triangles, red line; red bars), or 10 mg/kg of (+)-CBD-HPE-STZ (white squares, dotted line; white bars). (b) Non-fasting blood glucose (BG) was monitored daily and (c) fasting blood glucose after 6 days of treatment. IPGTT was performed after 6 days of treatment, (d) blood glucose measured, and (e) area under the curve calculated. N = 6–7 mice/group. (f) Representative photomicrographs (20X) of insulin (green) and nuclei (DAPI, blue) staining of the pancreas. The scale bar is 50 μm. Quantification of (g) intra-islet staining, (h) beta cell mass per islet, and (i) average islet area. N = 100 islets/group, N = 6 mice/group for Vehicle-Cit. Bf. and (+)-CBD-HPE-STZ groups and N = 7 mice/group for Vehicle-STZ. Results are mean ± SEM. Significance when *p < 0.05, **p < 0.01 and ***p < 0.001 *versus* vehicle-citrate buffer-treated mice, $^{\#}$p < 0.05, $^{\#\#}$p < 0.01 and $^{\#\#\#}$p < 0.001 *versus* vehicle-STZ.

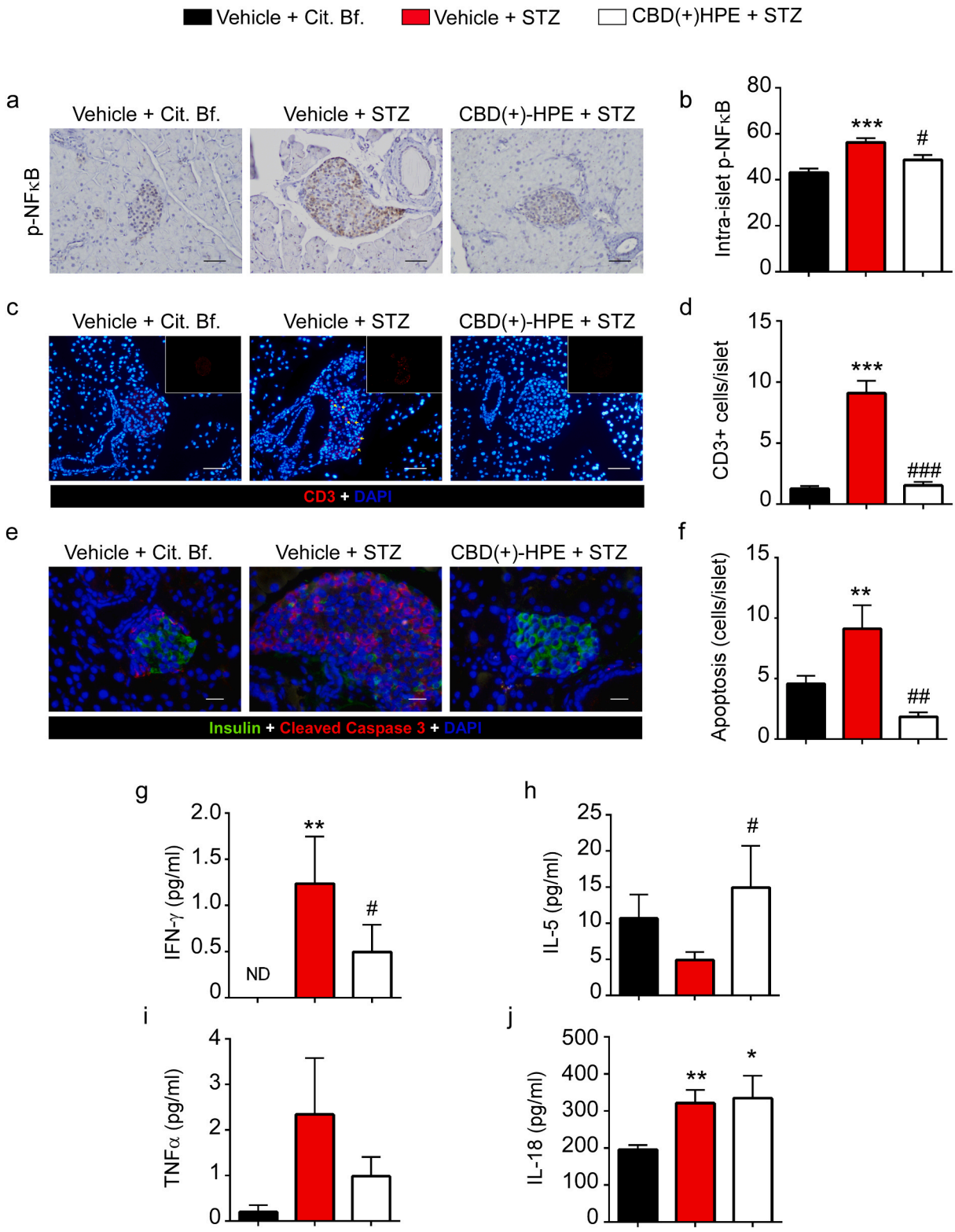

Fig. 4. (+)-CBD-HPE prevents STZ-induced beta cell apoptosis and ameliorates inflammation. Representative photomicrographs (20X), and quantification, of pancreas immunostaining for (a-b) of p-NF-κB-DAB, (c-d) CD3 (red) and nuclei (DAPI, blue), and (e-f) cleaved caspase 3 (red), insulin (green), and nuclei (DAPI, blue) in vehicle-citrate buffer- (Vehicle-Cit. Bf.; black bars), vehicle-STZ- (red bars) and (+)-CBD-HPE-STZ-treated mice (white bars) mice. The scale bar is 50 μm. N = 100 islets/group, N = 6 mice/group for Vehicle-Cit. Bf. and (+)-CBD-HPE-STZ groups and N = 7 mice/group for Vehicle-STZ. Quantification of plasma (g) IFN-γ, (h) IL-5, (i) TNF-α and (j) IL-18 by ELISA. N = 6–7 mice/group. Results are mean ± SEM. Significance when *p < 0.05, **p < 0.01 and ***p < 0.001 *versus* vehicle-citrate buffer-treated mice, $^{\#}$p < 0.05, $^{\#\#}$p < 0.01 and $^{\#\#\#}$p < 0.001 *versus* vehicle-STZ-treated mice.

prevented STZ-induced insulitis (Fig. 4C-D). STZ further induced beta cell apoptosis, determined by a 2-fold increase in intra-islet cleaved caspase 3 staining compared to healthy control (Fig. 4E-F). Treatment with (+)-CBD-HPE completely avoided STZ-mediated beta cell death (Fig. 4E-F). It has been previously described that cannabinoids can regulate GLUT2, which is responsible for STZ toxicity [21,22]. We found no significant differences between vehicle and (+)-CBD-HPE-treated mice in GLUT2 levels in islets (Supplementary Fig. 2A-B).

Plasma levels of IFN-γ were undetectable in healthy control, and treatment with STZ significantly increased their levels (Fig. 4G).

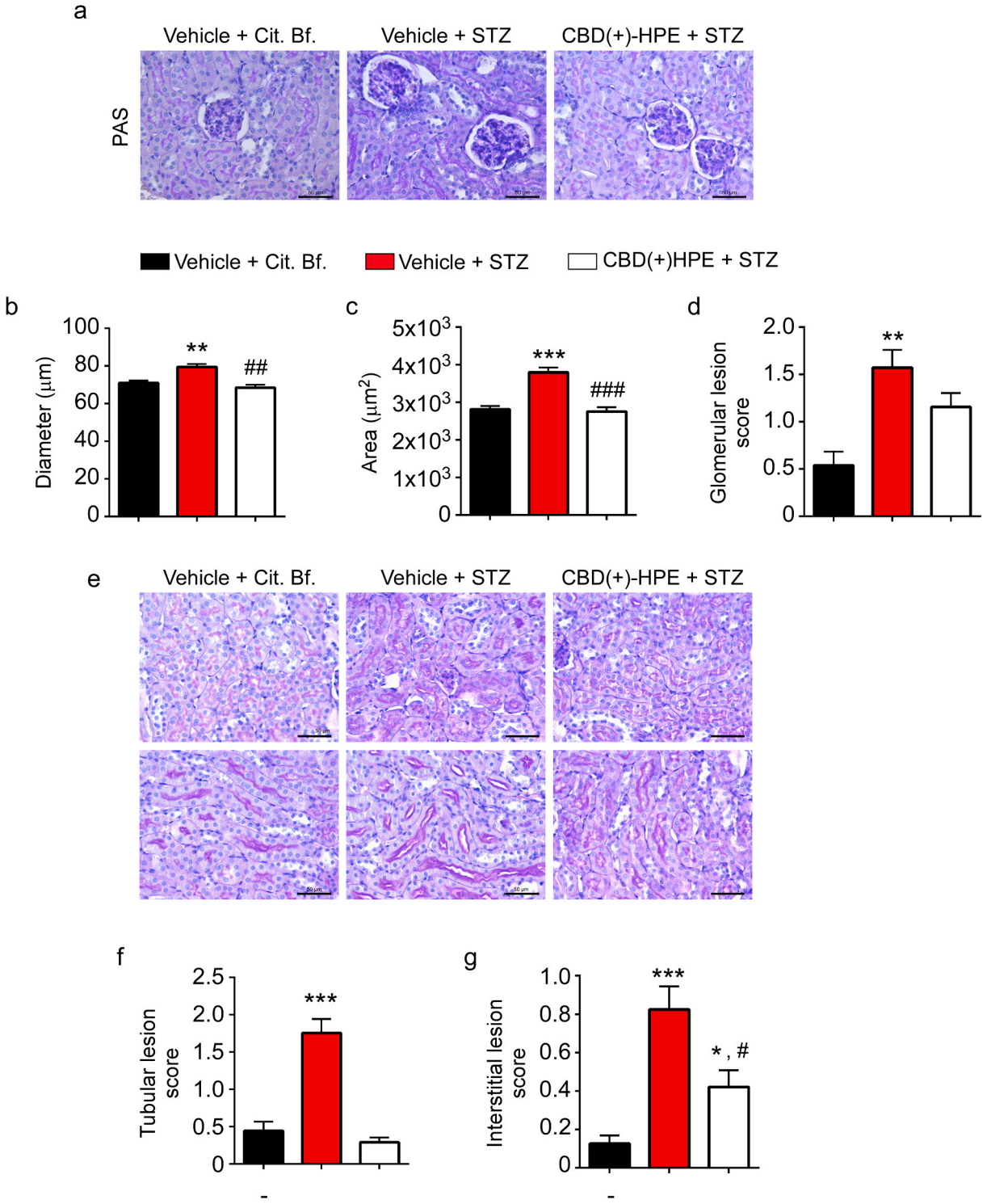

Fig. 5. (+)-CBD-HPE averts diabetic nephropathy. Representative photomicrographs (10X) of (a) glomerulus from vehicle-citrate buffer- (Vehicle-Cit. Bf.; black bars), vehicle-STZ- (red bars) and (+)-CBD-HPE-STZ-treated mice (white bars) kidney stained with PAS. Quantification of glomerulus (b) diameter, (c) area, and (d) glomerular lesion score. (e) Representative photomicrographs (10X) and quantification of (f) tubular and (g) interstitial lesion score from vehicle-citrate buffer- (Vehicle-Cit. Bf.; black bars), vehicle-STZ- (red bars) and (+)-CBD-HPE-STZ-treated mouse (white bars) kidneys stained with PAS. The scale bar is 50 µm. N = 20 images/group, N = 6 mice/group for Vehicle-Cit. Bf. and (+)-CBD-HPE-STZ groups and N = 7 mice/group for Vehicle-STZ. Results are mean ± SEM. Significance when *p < 0.05, **p < 0.01 and ***p < 0.001 *versus* vehicle-citrate buffer, $^{\#}$p < 0.05, $^{\#\#}$p < 0.01 and $^{\#\#\#}$p < 0.001 *versus* vehicle-STZ.

Treatment with (+)-CBD-HPE significantly reduced the levels of IFN-γ of 2.5 folds compared to STZ-treated mice (Fig. 4G). Treatment with (+)-CBD-HPE also significantly increased IL-5 levels of 3 folds compared to STZ-treated mice (Fig. 4H), suggesting a protective anti-inflammatory role against STZ damage. Levels of TNFα tended to increase only upon STZ treatment compared to healthy controls ($p = 0.07$) (Fig. 4I). Plasma levels of IL-18 were significantly higher in both STZ- and (+)-CBD-HPE-treated mice compared to healthy controls (Fig. 4J), suggesting that the protective role of (+)-CBD-HPE occurs by T cell rather than macrophage modulation.

3.5. (+)-CBD-HPE prevents STZ-induced renal injury

Previous studies demonstrate that targeting the cannabinoid receptors alleviates renal injury [12,23,24]. We assayed kidney samples histologically by PAS staining to determine morphological changes in the glomerulus, tubules, and interstitium of diabetic mice compared to healthy controls. STZ induced glomerular morphological changes, as reflected by an increase in glomerulus diameter and area (Fig. 5A-C). STZ also significantly increased the glomerular lesion score, *i.e.* increased in hypercellularity, mesangial matrix lesions, and capillary dilatation, of 2.9 folds compared to healthy control (Fig. 5A, D). Treatment with (+)-CBD-HPE prevented the glomerular hypertrophy induced by STZ, as observed by a glomerular area and diameter comparable to healthy controls (Fig. 5A-C), and tended to, although it was not significantly ($p = 0.09$), reduce the glomerular lesions (Fig. 5A, D). STZ also induced significant degeneration and atrophy of tubules, with a 3.9-fold increase in tubular lesion score compared to healthy control (Fig. 5E-F). (+)-CBD-HPE prevented STZ-induced tubular lesions (Fig. 5E-F). STZ increased the interstitial lesion score, *i.e.* an increase in interstitial fibrosis and inflammation, of 6.8 folds compared to healthy controls (Fig. 5E, D), while treatment with (+)-CBD-HPE induced a significant 1.95-fold reduction of these lesions (Fig. 5E, D). As described previously [22], STZ induced a significant increase in GLUT2 levels in the kidney (Supplementary Fig. 2B-C). Treatment with (+)-CBD-HPE had no significant effect on renal GLUT2 levels ($p = 0.2$; supplementary Fig. 2B-C).

3.6. (+)-CBD-HPE prevents STZ-induced renal fibrosis and inflammation

In diabetic nephropathy, the overproduction of extracellular matrix is a feature of the disease that leads to inflammation and glomerular

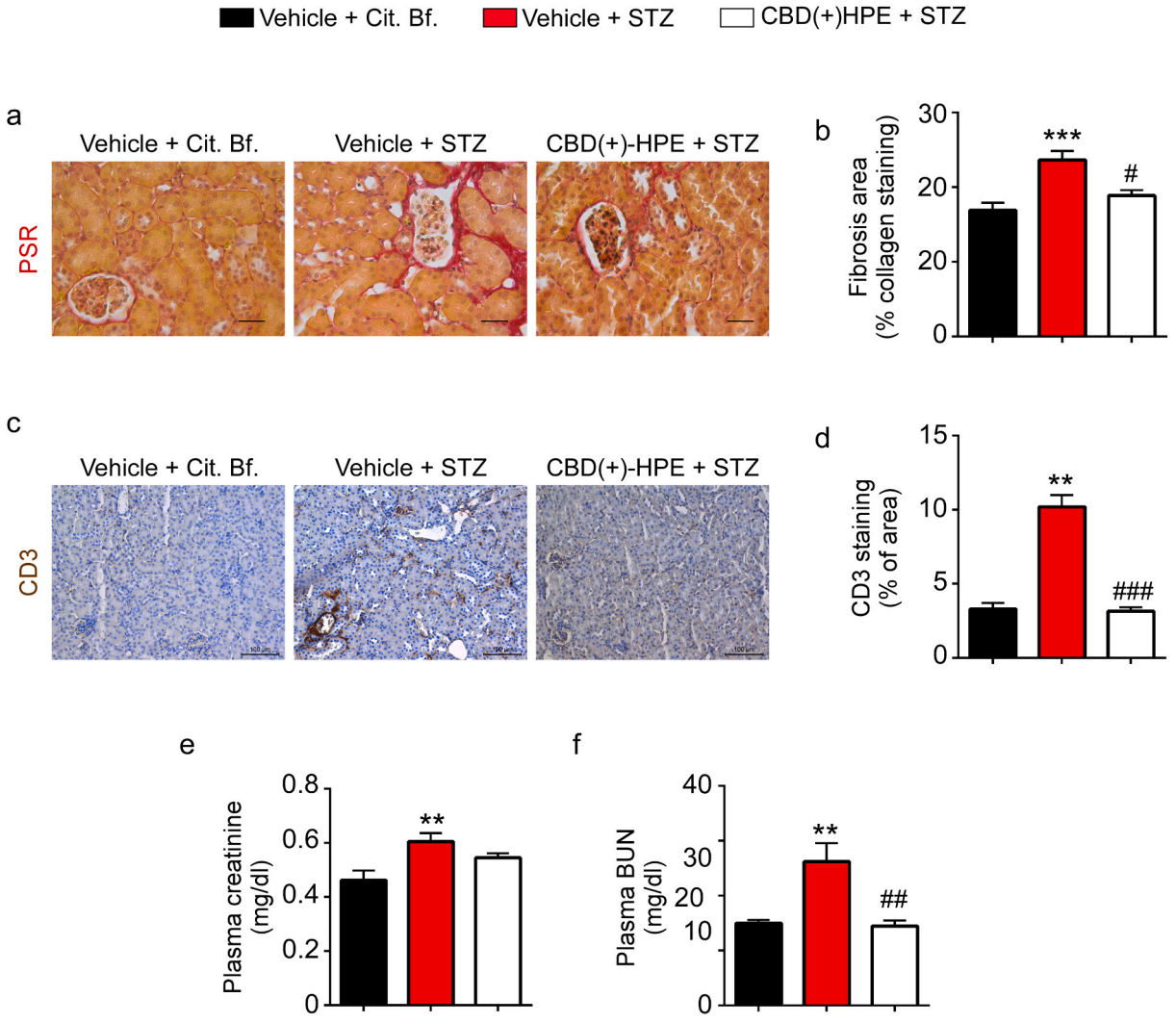

Fig. 6. (+)-CBD-HPE prevents fibrosis and inflammation in the kidney. Representative photomicrographs (10X), and quantification, of kidney stained for (a-b) PSR and (c-d) CD3-DAB from vehicle-citrate buffer- (Vehicle-Cit. Bf.; black bars), vehicle-STZ- (red bars) and (+)-CBD-HPE-STZ-treated mice (white bars). The scale bar is 50 μm. N = 20 images/group, N = 6 mice/group for Vehicle-Cit. Bf. and (+)-CBD-HPE-STZ groups and N = 7 mice/group for Vehicle-STZ. Quantification of (e) plasma creatinine and (f) BUN. N = 6 mice/group for Vehicle-Cit. Bf. and (+)-CBD-HPE-STZ groups and N = 7 mice/group for Vehicle-STZ. Results are mean ± SEM. Significance when $^{**}p < 0.01$ and $^{***}p < 0.001$ *versus* vehicle-citrate buffer, $^{\#}p < 0.05$, $^{\#\#}p < 0.01$ and $^{\#\#\#}p < 0.001$ *versus* vehicle-STZ.

sclerosis [25]. We determined renal fibrosis by PSR. PSR staining showed that STZ treatment led to a 1.4-fold increase of the fibrosis in glomeruli and interstitium compared to healthy controls (Fig. 6A-B). Treatment with (+)-CBD-HPE fully prevented STZ-induced renal fibrosis as observed by a significant reduction of PSR stained area compared to STZ-vehicle (Fig. 6A-B). Diabetic nephropathy was associated with recruitment and retention of lymphocytes, as shown by a significant increase of 3.1-fold in the $CD3^+$ stained area in the renal interstitium of STZ-vehicle compared to healthy controls (Fig. 6C-D). Treatment with (+)-CBD-HPE fully prevented the recruitment and/or retention of T lymphocytes as observed by CD3 staining (Fig. 6C-D).

Mice injected with STZ-vehicle, but not (+)-CBD-HPE-treated mice, presented a significantly increased level of creatinine in plasma compared to healthy controls (Fig. 6E). Also, treatment with STZ induced a significant increase in BUN compared to healthy controls (Fig. 6F), which was voided with (+)-CBD-HPE treatment (Fig. 6G).

4. Discussion

The phytocannabinoid (-)-trans CBD is a multitarget compound with different biomedical applications. Besides, (-)-CBD has been used as a template to develop novel chemical entities such as the aminoquinones VCE-004.3 and VCE-004.8 [26,27], and the later has been formulated as EHP-101 for oral delivery and a Phase II study in Systemic Sclerosis patients has been initiated (ClinicalTrials.gov: NCT04166552). In contrast, the synthetic enantiomer (+)-trans-CBD has been poorly explored. Herein, we confirmed that (+)-trans-CBD showed strong binding to CB_2R, and an enhanced affinity to CB_1R compared to (-)-trans-CBD. A further modification on position 2 of the resorcinol moiety led to (+)-CBD-HPE that showed a very potent binding activity on both CB_1R and CB_2R acting as a functional CB_1R antagonist and CB_2R agonist. A molecule with these characteristics is of pharmacological therapeutic interest considering the impact that targeting both receptors has in a plethora of metabolic and immune disorders. We have demonstrated (see [8] and present data) that (+)-enantiomers of CBD and derivatives exhibit a strong elevation of their affinities and intrinsic activities at both cannabinoid receptors, showing their potential as new experimental tools for research and, even, for therapeutic development, a fact investigated in the second part of this study. A potential transformation of (+)-enantiomers in the (-)-forms by intracellular racemases and *vice-versa* may represent an important follow-up objective to be investigated, given that it may enhance or reduce their biological effects. This is something relevant to be investigated, but it is unlikely that it happened in our binding analysis conducted with commercial membranes, since there is only the receptor of interest. By contrast, racemization might happen in our cell-based and *in vivo* assays, but, in that case, the result would be a reduction in the biological effect of the (+)-CBD-HPE, which was not found in our study.

The synthesis of (+)-CBD and (+)-CBD-HPE is similar to the widely known synthetic route for preparations of the natural occurring (-)-CBD [28]. Olivetol methyl ester and the respective terpene (4S-menthadienoles for (+)-CBD derivatives) undergo a Friedel Craft alkylation to the respective Cannabidiol carboxylic methyl ester. The respective ester is subsequently saponified to the crystalline (+)-CBD. (+)-CBD-HPE could be prepared by transesterification of the (+)-CBD methyl ester with the appropriate alcohol. This transesterification can be done with the majority of known organic alcohols, which opens up a near-infinite number of future new (+)-CBD derivatives with novel pharmaceutical applications.

Contrary to the synthesis of naturally occurring (-)-CBD, there is a problem of enantiomeric purity. 4R-menthadienols or their precursors (*e.g.* (-)-limonene) are not readily naturally available in enantiomeric pure compositions or have to be prepared with an increased technical effort. This necessitates, for compounds like (+)-CBD-HPE, either enantiomeric pure starting materials or an expensive and time-consuming chiral purification method. (+)-CBD however tolerates a 4S-menthadienol starting material with up to 5% (-)-CBD. This is due to the (+)-CBDs crystalline characteristic, which enables the here discussed purification by crystallization to isolate (+)-CBD with an enantiomeric excess of 99% from a mixture of (-)- and (+)-CBD. Hence, we obtained a compound highly-pure and with a pharmaceutical profile for cannabinoid receptors that made it highly interesting for its therapeutic application.

The CB_1R plays a key role in type 2 diabetic nephropathy. Indeed, CB_1R is overactive in this pathology [12], and its deletion in podocytes prevents diabetic nephropathy in obesity [23]. Here we show that (+)-CBD-HPE is a strong CB_1R antagonist, and it is plausible that its positive effect on the kidney depends on the antagonism of this receptor. Previously it has been shown that pharmacological blockers of CB_1R were promising therapeutics for diabetic nephropathy [29,30]. CB_1R, located in the proximal tubule, when overactivated as it occurs in obesity, plays a key role in the activation of inflammation and the development of renal fibrosis [30]. Blockade of CB_1R was able to prevent chronic inflammation and also to significantly reduce renal fibrosis, preserving kidney function. In T1D, similarly to type 2, hyperglycemia causes hypertension, oxidative stress, and inflammation that chronically leads to renal damage, and blockade of the CB_1R seems to be therapeutic. Specifically, CB_1R was described to regulate GLUT2 recirculation in the kidney of T1D rodents, thus impacting on glucose absorbance and renal injury and dysfunction [22]. However, treatment with (+)-CBD-HPE was not able to restore the levels of GLUT2, suggesting that (+)-CBD-HPE is reducing inflammation and fibrosis without altering glucose transportation. We also show that (+)-CBD-HPE acts, dually, as an agonist of the CB_2R, a cannabinoid receptor that plays an important role in immune cell regulation. Other dual-acting drugs have been shown to effectively prevent nephropathy in rodents. A double CB_1R antagonist and iNOS agonist prevented inflammation, fibrosis, oxidative stress, and thus renal damage in obese mice [30]. Here we show that a novel dual-acting drug, that blocks CB_1R and simultaneously activates CB_2R efficiently avert T1D and its associated renal complications. The action of (+)-CBD-HPE on CB_2R can also, by itself, significantly reduce the inflammation that eventually leads to tissue fibrosis. In fact, another CB_2R agonist, LEI-101, prevented cisplatin-mediated kidney damage and dysfunction by reducing both oxidative stress and inflammation within the tissue [31]. A more recent study showed that activation of CB_2R enhances renal vascularization thus enhancing renal perfusion in a CB_1R-independent manner [32]. However, a CB_2R inverse agonist, XL-001, has also been shown to prevent fibrogenesis, and CB_2R knockout mice are protected against renal fibrosis [33], contrary to the findings of Dr. Mukhopadhyay et al. Despite these discrepancies, that can be explained by the differences in the models of study, drug-toxicity based *vs* unilateral ureteral obstruction, our findings show that a dual acting CB_1R antagonist and CB_2R agonist is able to prevent renal inflammation and fibrosis in a mouse model of T1D, and that the benefit includes lower inflammation, thus less morphological changes and fibrosis, leading to preservation of kidney function.

Damage induced by STZ in the pancreas includes oxidative stress and activation of the inflammatory response, leading to apoptosis of beta cells. Eventual beta cell mass loss because of STZ causes loss of circulating insulin, hence hyperglycemia. CBD has been shown to delay the onset of T1D in non-obese diabetic mice, although the mechanism of this observation is unknown. We found that (+)-CBD-HPE ameliorated beta cell mass loss because of STZ by greatly reducing islet inflammation and T cells infiltration into the islets. Moreover, (+)-CBD-HPE prevented STZ-induced beta cell apoptosis. The blockade of CB_1R has been shown to enhance beta cell function [21,34,35]. In another model of metabolic disorder, genetic ablation of CB_1R in beta cells (*i.e.* "blockade" of CB_1R) leads to an inhibition of the inflammasome in islets, preventing the activation of NF-κB and, consequently, voiding immune cells infiltration in and around the islets [14]. Hence, blockade of CB_1R is a therapeutic approach to preserve beta cell mass and function. In fact, CB_1R, by directly binding to the insulin receptor in beta cells, modulates its

downstream signal, acting, when overactivated, as an inducer of beta cell apoptosis through the Akt pathway [36]. Thus, (+)-CBD-HPE may be preserving beta cells by blocking CB_1R, reducing both beta cell inflammation and apoptosis. Moreover, defects on CB_2R signaling leads to incapability to suppress T cell proliferation, increasing the risk of immune-related disorders (reviewed in [37]). Of note, (+)-CBD-HPE reduced the pro-inflammatory cytokines IFN-γ and TNFα, while increasing the IL-5, indicating that it may be acting as an anti-inflammatory compound at the T cell level by altering the Th1/Th2 ratio. The phytocannabinoid THC significantly reduces Th1 cytokine production while enhancing the production of cytokines characteristic of Th2 cells in human leukocytes, in a CB_2R-dependent manner [38]. In line with these observations, a dual CB_1R-antagonist CB_2R agonist such as (+)-CBD-HPE is a good candidate for the treatment of T1D to preserve beta cell mass and protect from islet inflammation and insulitis. It is also important to emphasize that this protection of the pancreatic beta cells and prevention of the inflammatory damage induced by STZ could also be behind the nephroprotective mechanism of renal protection. However, previous studies showed that targeting of CB_1R and CB_2R in diabetic mice is a promising strategy for the treatment of diabetic nephropathy. When given in combination, the CB1R antagonist AM6545 and the CB2R agonist AM1241 to STZ-induced diabetic mice, they exert a synergic effect on renal protection [39]. Further *in vitro* studies, as well as *in vivo* studies in already diabetic mice are warranted to further investigate the nephroprotective capacity of (+)-CBD-HPE. In addition, the potential effect of both (+)-CBD and (+)-CBD-HPE on other (-)-CBD targets such as GPR55, Adenosine receptors, 5-HT1A, 5-HT2A or PPARγ need to investigated for a further characterization of these compounds.

Various pharmacological strategies to safely target the cannabinoid receptors have been taking place since the 2000's after the Rimonabant fiasco despite its multiple beneficial effects due to its action on the central nervous system [40]. In this sense, peripherally-acting as well as more specific drugs have been developed [41]. Recently, dual-acting drugs have been suggested and proven to be a strong approach to add another level of specificity and safety [42]. However, due to the dark past of CB1R blockade, tissue distribution and behavioral studies will be necessary for the translational value of (+)-CBD-HPE.

5. Conclusions

Herein we show a methodology by which highly pure (+)-enantiomers of CBD are synthesized, and whose affinities and activities at both cannabinoid receptors CB_1R and CB_2R are strongly enhanced. In particular, we showcased a promising molecule, (+)-CBD-HPE, that has a strong affinity for both receptors, and that acts as an antagonist of CB_1R and as an agonist of CB_2R. The relevance of such a compound has been already highlighted in the field, despite the structural difficulties to acquire potent ligand for both receptors [42]. Moreover, we demonstrate that the pharmacological profile of (+)-CBD-HPE has a promising potential to be used for metabolic and immune-related disorders, as are diabetes and its complications such as diabetic nephropathy.

CRediT authorship contribution statement

IGM, BLM, and EM: Participated in the conception and design of the study; **MW**: Designed and performed the chemical synthesis of cannabinoids; **IGM, BCH, AE, SYRZ and FJBM**: Acquired, analyzed, and interpreted the *in vivo* data. **JDUB, MGC, JFR, and JAC:** Acquired, analyzed, and interpreted the *in vitro* data. **IGM and EM:** wrote the article. All authors were involved in drafting and revising the article.

Acknowledgements

IGM was funded by the Consejeria de Salud y Familias of Junta de Andalucia - Proyectos de Investigación en Salud [PI-0318-2018] and Nicolas Monardes Program, Spain [C1-0018-2019]. This work was also partially supported by grants SAF2017-87701-R to EM from the Ministry of the Economy and Competition, Spain (MINECO) co-financed with the European Union FEDER funds, and RTI2018-098885-B-100 to JFR from the Ministry of Science, Innovation and University, Spain (MICIU). Emerald Health Biotechnology España SLU and Symrise AG also supported this work and had no further role in study design, the collection, analysis, and interpretation of data, in the writing of the report, or in the decision to submit the paper for publication.

Conflict of Interest

BCH and JDUB are employees of Emerald Health Biotechnology, MW is an employee of Symrise AG and submitted a PCT (PCT/EP2018/067366) describing the synthesis of (+)-CBD and (+)-CBD-HPE. EM is a member of the Scientific Advisory Board of Emerald Health. Other authors declare no conflicts of interest.

Appendix A. Supporting information

Supplementary data associated with this article can be found in the online version at doi:10.1016/j.phrs.2021.105492.

References

[1] H. Li, Y. Liu, D. Tian, L. Tian, X. Ju, L. Qi, Y. Wang, C. Liang, Overview of cannabidiol (CBD) and its analogues: structures, biological activities, and neuroprotective mechanisms in epilepsy and Alzheimer's disease, Eur. J. Med. Chem. 192 (2020), 112163, https://doi.org/10.1016/j.ejmech.2020.112163.
[2] S. Giacoppo, P. Bramanti, E. Mazzon, Sativex in the management of multiple sclerosis-related spasticity: an overview of the last decade of clinical evaluation, Mult. Scler. Relat. Disord. 17 (2017) 22–31, https://doi.org/10.1016/j.msard.2017.06.015.
[3] K. Sekar, A. Pack, Epidiolex as adjunct therapy for treatment of refractory epilepsy: a comprehensive review with a focus on adverse effects, F1000Research 8 (2019), https://doi.org/10.12688/f1000research.16515.1.
[4] R.B. Laprairie, A.M. Bagher, M.E.M. Kelly, E.M. Denovan-Wright, Cannabidiol is a negative allosteric modulator of the cannabinoid CB1 receptor, Br. J. Pharmacol. 172 (2015) 4790–4805, https://doi.org/10.1111/bph.13250.
[5] T. Bisogno, L. Hanuš, L. De Petrocellis, S. Tchilibon, D.E. Ponde, I. Brandi, A. S. Moriello, J.B. Davis, R. Mechoulam, V. Di Marzo, Molecular targets for cannabidiol and its synthetic analogues: effect on vanilloid VR1 receptors and on the cellular uptake and enzymatic hydrolysis of anandamide, Br. J. Pharm. 134 (2001) 845–852, https://doi.org/10.1038/sj.bjp.0704327.
[6] E. Fride, C. Feigin, D.E. Ponde, A. Breuer, L. Hanuš, N. Arshavsky, R. Mechoulam, (+)-Cannabidiol analogues which bind cannabinoid receptors but exert peripheral activity only, Eur. J. Pharmacol. 506 (2004) 179–188, https://doi.org/10.1016/j.ejphar.2004.10.049.
[7] L.O. Hanuš, S. Tchilibon, D.E. Ponde, A. Breuer, E. Fride, R. Mechoulam, Enantiomeric cannabidiol derivatives: Synthesis and binding to cannabinoid receptors, Org. Biomol. Chem. 3 (2005) 1116–1123, https://doi.org/10.1039/b416943c.
[8] M.R. Götz, J.A. Collado, J. Fernández-Ruiz, B.L. Fiebich, L. García-Toscano, M. Gómez-Cañas, O. Koch, A. Leha, E. Muñoz, C. Navarrete, M.R. Pazos, U. Holzgrabe, Structure–effect relationships of novel semi-synthetic cannabinoid derivatives, Front. Pharmacol. 10 (2019) 1284, https://doi.org/10.3389/fphar.2019.01284.
[9] L. Jacobsen, D. Schatz, Current and future efforts toward the prevention of type 1 diabetes, Pediatr. Diabetes 17 (2016) 78–86, https://doi.org/10.1111/pedi.12333.
[10] N.G. Forouhi, N.J. Wareham, Epidemiology of diabetes, Medicine Baltim. 42 (2014) 698–702, https://doi.org/10.1016/j.mpmed.2014.09.007.
[11] L. Weiss, M. Zeira, S. Reich, S. Slavin, I. Raz, R. Mechoulam, R. Gallily, Cannabidiol arrests onset of autoimmune diabetes in NOD mice, Neuropharmacology 54 (2008) 244–249, https://doi.org/10.1016/j.neuropharm.2007.06.029.
[12] T. Jourdan, G. Szandaa, A.Z. Rosenberg, J. Tam, B.J. Earley, G. Godlewski, R. Cinar, Z. Liu, J. Liu, C. Ju, P. Pacher, G. Kunos, Overactive cannabinoid 1 receptor in podocytes drives type 2 diabetic nephropathy, Proc. Natl. Acad. Sci. USA (2014) E5420–E5428, https://doi.org/10.1073/pnas.1419901111.
[13] T. Jourdan, G. Godlewski, R. Cinar, A. Bertola, G. Szanda, J. Liu, J. Tam, T. Han, B. Mukhopadhyay, M.C. Skarulis, C. Ju, M. Aouadi, M.P. Czech, G. Kunos, Activation of the Nlrp3 inflammasome in infiltrating macrophages by endocannabinoids mediates beta cell loss in type 2 diabetes, Nat. Med. 19 (2013) 1132–1140, https://doi.org/10.1038/nm.3265.
[14] I. González-Mariscal, R.A. Montoro, M.E. Doyle, Q.-R. Liu, M. Rouse, J. F. O'Connell, S. Santa-Cruz Calvo, S.M. Krzysik-Walker, S. Ghosh, O.D. Carlson, E. Lehrmann, Y. Zhang, K.G. Becker, C.W. Chia, P. Ghosh, J.M. Egan, Absence of cannabinoid 1 receptor in beta cells protects against high-fat/high-sugar diet-induced beta cell dysfunction and inflammation in murine islets, Diabetologia 61 (2018) 1470–1483, https://doi.org/10.1007/s00125-018-4576-4.

[15] V. Katchan, P. David, Y. Shoenfeld, Cannabinoids and autoimmune diseases: a systematic review, Autoimmun. Rev. 15 (2016) 513–528, https://doi.org/10.1016/J.AUTREV.2016.02.008.
[16] M. Gómez-Cañas, P. Morales, L. García-Toscano, C. Navarrete, E. Muñoz, N. Jagerovic, J. Fernández-Ruiz, M. García-Arencibia, M.R. Pazos, Biological characterization of PM226, a chromenoisoxazole, as a selective CB2 receptor agonist with neuroprotective profile, Pharmacol. Res. 110 (2016) 205–215, https://doi.org/10.1016/j.phrs.2016.03.021.
[17] M.C. Deeds, J.M. Anderson, A.S. Armstrong, D.A. Gastineau, H.J. Hiddinga, A. Jahangir, N.L. Eberhardt, Y.C. Kudva, Single dose streptozotocin-induced diabetes: considerations for study design in islet transplantation models, Lab. Anim. 45 (2011) 131–140, https://doi.org/10.1258/la.2010.010090.
[18] T.D. Hewitson, E.R. Smith, C.S. Samuel, Qualitative and quantitative analysis of fibrosis in the kidney, Nephrology 19 (2014) 721–726, https://doi.org/10.1111/nep.12321.
[19] C.O. Eleazu, K.C. Eleazu, S. Chukwuma, U.N. Essien, Review of the mechanism of cell death resulting from streptozotocin challenge in experimental animals, its practical use and potential risk to humans, J. Diabetes Metab. Disord. 12 (2013) 60, https://doi.org/10.1186/2251-6581-12-60.
[20] D. Melloul, Role of NF-kappaB in beta-cell death, Biochem. Soc. Trans. 36 (2008) 334–339, https://doi.org/10.1042/BST0360334.
[21] H. Shin, J.H. Han, J. Yoon, H.J. Sim, T.J. Park, S. Yang, E.K. Lee, R.N. Kulkarni, J. M. Egan, W. Kim, Blockade of cannabinoid 1 receptor improves glucose responsiveness in pancreatic beta cells, J. Cell. Mol. Med. 22 (2018) 2337–2345, https://doi.org/10.1111/jcmm.13523.
[22] L. Hinden, S. Udi, A. Drori, A. Gammal, A. Nemirovski, R. Hadar, S. Baraghithy, A. Permyakova, M. Geron, M. Cohen, S. Tsytkin-Kirschenzweig, Y. Riahi, G. Leibowitz, Y. Nahmias, A. Priel, J. Tam, Modulation of renal GLUT2 by the cannabinoid-1 receptor: implications for the treatment of diabetic nephropathy, J. Am. Soc. Nephrol. 29 (2018) 434–448, https://doi.org/10.1681/ASN.2017040371.
[23] T. Jourdan, J.K. Park, Z.V. Varga, J. Pálóczi, N.J. Coffey, A.Z. Rosenberg, G. Godlewski, R. Cinar, K. Mackie, P. Pacher, G. Kunos, Cannabinoid-1 receptor deletion in podocytes mitigates both glomerular and tubular dysfunction in a mouse model of diabetic nephropathy, Diabetes Obes. Metab. 20 (2018) 698–708, https://doi.org/10.1111/dom.13150.
[24] F. Barutta, S. Grimaldi, I. Franco, S. Bellini, R. Gambino, S. Pinach, A. Corbelli, G. Bruno, M.P. Rastaldi, T. Aveta, E. Hirsch, V. Di Marzo, G. Gruden, Deficiency of cannabinoid receptor of type 2 worsens renal functional and structural abnormalities in streptozotocin-induced diabetic mice, Kidney Int. 86 (2014) 979–990, https://doi.org/10.1038/ki.2014.165.
[25] P. Boor, J. Floege, Chronic kidney disease growth factors in renal fibrosis, Clin. Exp. Pharmacol. Physiol. 38 (2011) 441–450, https://doi.org/10.1111/j.1440-1681.2011.05487.x.
[26] C. del Rio, I. Cantarero, B. Palomares, M. Gómez-Cañas, J. Fernández-Ruiz, C. Pavicic, A. García-Martín, M. Luz Bellido, R. Ortega-Castro, C. Pérez-Sánchez, C. López-Pedrera, G. Appendino, M.A. Calzado, E. Muñoz, VCE-004.3, a cannabidiol aminoquinone derivative, prevents bleomycin-induced skin fibrosis and inflammation through PPARγ- and CB $_2$ receptor-dependent pathways, Br. J. Pharmacol. 175 (2018) 3813–3831, https://doi.org/10.1111/bph.14450.
[27] C. Del Río, C. Navarrete, J.A. Collado, M.L. Bellido, M. Gómez-Cañas, M.R. Pazos, J. Fernández-Ruiz, F. Pollastro, G. Appendino, M.A. Calzado, I. Cantarero, E. Muñoz, The cannabinoid quinol VCE-004.8 alleviates bleomycin-induced scleroderma and exerts potent antifibrotic effects through peroxisome proliferator-activated receptor-γ and CB2 pathways, Sci. Rep. 6 (2016) 1–14, https://doi.org/10.1038/srep21703.
[28] O. Koch, M. Götz, J. Looft, T. Vössing, Mixtures of cannabinoid compounds, their preparation and use: (−)-trans-Cannabidiol, Tetrahydrocannabidiol and their derivatives. EP2842933B1, EP2842933B1, 2015.
[29] S. Udi, L. Hinden, M. Ahmad, A. Drori, M.R. Iyer, R. Cinar, M. Herman-Edelstein, J. Tam, Dual inhibition of cannabinoid CB1 receptor and inducible NOS attenuates obesity-induced chronic kidney disease, Br. J. Pharmacol. 177 (2020) 110–127, https://doi.org/10.1111/bph.14849.
[30] S. Udi, L. Hinden, B. Earley, A. Drori, N. Reuveni, R. Hadar, R. Cinar, A. Nemirovski, J. Tam, Proximal tubular cannabinoid-1 receptor regulates obesity-induced CKD, J. Am. Soc. Nephrol. 28 (2017) 3518–3532, https://doi.org/10.1681/ASN.2016101085.
[31] P. Mukhopadhyay, M. Baggelaar, K. Erdelyi, Z. Cao, R. Cinar, F. Fezza, B. Ignatowska-Janlowska, J. Wilkerson, N. Van Gils, T. Hansen, M. Ruben, M. Soethoudt, L. Heitman, G. Kunos, M. Maccarrone, A. Lichtman, P. Pacher, M. Van Der Stelt, The novel, orally available and peripherally restricted selective cannabinoid CB2 receptor agonist LEI-101 prevents cisplatin-induced nephrotoxicity, Br. J. Pharmacol. 173 (2016) 446–458, https://doi.org/10.1111/bph.13338.
[32] J.D. Pressly, H. Soni, S. Jiang, J. Wei, R. Liu, B.M. Moore, A. Adebiyi, F. Park, Activation of the cannabinoid receptor 2 increases renal perfusion, Physiol. Genom. 51 (2019) 90–96, https://doi.org/10.1152/physiolgenomics.00001.2019.
[33] L. Zhou, S. Zhou, P. Yang, Y. Tian, Z. Feng, X.Q. Xie, Y. Liu, Targeted inhibition of the type 2 cannabinoid receptor is a novel approach to reduce renal fibrosis, Kidney Int. 94 (2018) 756–772, https://doi.org/10.1016/j.kint.2018.05.023.
[34] I. González-Mariscal, S.M. Krzysik-Walker, W. Kim, M. Rouse, J.M. Egan, Blockade of cannabinoid 1 receptor improves GLP-1R mediated insulin secretion in mice, Mol. Cell. Endocrinol. 423 (2016) 1–10, https://doi.org/10.1016/j.mce.2015.12.015.
[35] I. González-Mariscal, S.M. Krzysik-Walker, M.E. Doyle, Q.-R. Liu, R. Cimbro, S. Santa-Cruz Calvo, S. Ghosh, Ł. Cieśla, R. Moaddel, O.D. Carlson, R.P. Witek, J. F. O'Connell, J.M. Egan, Human CB1 receptor isoforms, present in hepatocytes and β-cells, are involved in regulating metabolism. Sci. Rep. 6 (2016) 33302, https://doi.org/10.1038/srep33302.
[36] W. Kim, Q. Lao, Y.-K. Shin, O.D. Carlson, E.K. Lee, M. Gorospe, R.N. Kulkarni, J. M. Egan, Cannabinoids induce pancreatic β-cell death by directly inhibiting insulin receptor activation, Sci. Signal. 5 (2012) 23, https://doi.org/10.1126/scisignal.2002519.
[37] A. Oláh, Z. Szekanecz, T. Bíró, Targeting cannabinoid signaling in the immune system: "high"-ly exciting questions, possibilities, and challenges, Front. Immunol. 8 (2017) 1487, https://doi.org/10.3389/fimmu.2017.01487.
[38] M. Yuan, S.M. Kiertscher, Q. Cheng, R. Zoumalan, D.P. Tashkin, M.D. Roth, Δ9-Tetrahydrocannabinol regulates Th1/Th2 cytokine balance in activated human T cells, J. Neuroimmunol. 133 (2002) 124–131, https://doi.org/10.1016/S0165-5728(02)00370-3.
[39] F. Barutta, S. Grimaldi, R. Gambino, K. Vemuri, A. Makriyannis, L. Annaratone, V. Di Marzo, G. Bruno, G. Gruden, Dual therapy targeting the endocannabinoid system prevents experimental diabetic nephropathy, Nephrol. Dial. Transpl. 32 (2017) 1655–1665, https://doi.org/10.1093/ndt/gfx010.
[40] R. Christensen, P.K. Kristensen, E.M. Bartels, H. Bliddal, A. Astrup, Efficacy and safety of the weight-loss drug rimonabant: a meta-analysis of randomised trials, Lancet 370 (2007) 1706–1713, https://doi.org/10.1016/S0140-6736(07)61721-8.
[41] G. Kunos, D. Osei-Hyiaman, S. Batkai, K.A. Sharkey, A. Makriyannis, Should peripheral CB(1) cannabinoid receptors be selectively targeted for therapeutic gain? Trends Pharmacol. Sci. 30 (2009) 1–7, https://doi.org/10.1016/j.tips.2008.10.001S0165-6147(08)00245-9.
[42] R. Cinar, M.R. Iyer, G. Kunos, The therapeutic potential of second and third generation CB1R antagonists, Pharmacol. Ther. 208 (2020), 107477, https://doi.org/10.1016/j.pharmthera.2020.107477.